Circulating Plasma Extracellular Vesicles from Septic Mice Induce Inflammation via MicroRNA- and TLR7-Dependent Mechanisms

Jinjin Xu,*,† Yan Feng,* Anjana Jeyaram,‡ Steven M. Jay,‡ Lin Zou,* and Wei Chao*

We have previously reported that a group of host cellular microRNAs (miRNAs; miR-34a-5p, miR-122-5p, miR-145-5p, miR-146a-5p, miR-210-3p) are released into the blood during sepsis, some of which are capable of inducing complement activation, cytokine production, and leukocyte migration. Extracellular vesicles (EVs) have been proposed as vehicles for extracellular miRNA-mediated intercellular communication. However, the biological function of plasma EVs and the associated miRNAs in sepsis are largely unknown. In this study, we tested the hypothesis that plasma EVs in sepsis are proinflammatory and EV-associated miRNAs are responsible for EV-induced cytokine production. Compared with those of sham mice, the plasma EVs from septic mice were slightly smaller (157 ± 2 versus 191 ± 6 nm, $p < 0.0001$), but more abundant [$(1.6 \pm 0.14) \times 10^{10}$ versus $(0.93 \pm 0.14) \times 10^{10}$/ml plasma, $p < 0.003$]. miRNA array revealed that among 65 miRNAs, 8 miRNAs exhibited >1.5-fold increase in septic EVs compared with sham EVs, including miR-126-3p, miR-122-5p, miR-146a-5p, miR-145-5p, miR-26a-5p, miR-150-5p, miR-222-3p, and miR-181a-5p. Septic but not sham EVs were proinflammatory, promoting IL-6, TNF-α, IL-1β, and MIP-2 production. The effects of EVs were resistant to polymyxin B (an endotoxin inhibitor) but significantly inhibited by anti-miR inhibitors against miR-34a, miR-122, and miR-146a. Moreover, the septic EV-induced cytokine production was attenuated in TLR7$^{-/-}$ or MyD88$^{-/-}$ cells but remained the same in TLR3$^{-/-}$ or Trif$^{-/-}$ cells. In vivo, mice i.p. injected with septic EVs had marked peritoneal neutrophil migration, which was significantly attenuated in MyD88$^{-/-}$ mice. Taken together, these data demonstrate that plasma EVs of septic animals play an important role in inflammation, and EV-associated miRNAs likely mediate the cytokine production via TLR7-MyD88 signaling. ***The Journal of Immunology*****, 2018, 201: 3392–3400.**

Sepsis is a serious clinical condition with life-threatening organ dysfunction caused by a dysregulated host response to infection (1). It is the leading cause of death in the intensive care unit. Sepsis results in over 265,000 deaths per year in the United States, and the number of sepsis cases has continued to rise (2, 3). Although marked systemic inflammation is a hallmark of sepsis and plays a pivotal role in early sepsis pathogenesis, the molecular and cellular mechanisms that drive inflammation and subsequent organ injury are not fully understood.

Extracellular vesicles (EVs) are membrane-bound nanoparticles naturally released from almost every cell type in vivo and potentially play an important role in various diseases (4). Plasma EVs contain nucleotides, lipids, and proteins from the cells in which they originate, and in turn affect gene expression in recipient cells (5–7). For example, studies have shown that plasma EVs isolated from septic shock patients induce tissue expression of NO synthesis and NF-κB activation when injected into animals, demonstrating a proinflammatory effect (8).

MicroRNAs (miRNAs) are a group of small single-stranded noncoding RNAs that regulate gene expression by binding to the 3′ untranslated region of target mRNAs. Association of a miRNA with its mRNA target results in degradation of mRNA as well as inhibition of translation. Thus, by affecting gene translation in the cytoplasm, miRNAs act as regulators [generally gene repressors, but they can upregulate genes as well (9)], of a wide range of biological processes and play a critical role in health and diseases such as cardiovascular disorders (10–13). Importantly, recent studies have revealed that miRNAs also widely exist outside of cells in the blood circulation (14–17) and body fluids (18–20). These extracellular (ex) miRNAs are either packed in different

*Translational Research Program, Department of Anesthesiology and Center for Shock Trauma Anesthesiology Research, University of Maryland School of Medicine, Baltimore, MD 21201; †Department of Anesthesiology, Renmin Hospital of Wuhan University, Wuhan, Hubei 430060, People's Republic of China; and ‡Fischell Department of Bioengineering, University of Maryland, College Park, MD 20742

ORCIDs: 0000-0001-6154-9521 (J.X.); 0000-0002-2181-4367 (A.J.); 0000-0002-3827-5988 (S.M.J.); 0000-0002-2505-1360 (W.C.).

Received for publication July 19, 2018. Accepted for publication September 21, 2018.

This work was supported by National Institutes of Health Grants R01-GM097259 and R01-GM122908 (to W.C.) and R35-GM124775 (to L.Z.), a Shock Society Faculty Research Award (to L.Z.), a Frontiers in Anesthesia Research Award from the International Anesthesia Research Society (to W.C.), and National Natural Science Foundation of China Grant 8130162 (to J.X.).

The miRNA array data presented in this article have been submitted to the National Center for Biotechnology Information's Gene Expression Omnibus (https://www.ncbi.nlm.nih.gov/geo/query/acc.cgi?acc=GSE116829) under accession number GSE116829.

Address correspondence and reprint requests to Dr. Wei Chao and Dr. Lin Zou, Department of Anesthesiology and Center for Shock Trauma Anesthesiology Research, University of Maryland School of Medicine, 22 South Greene Street, Room S11-C10, Baltimore, MD 21201. E-mail addresses: wchao@som.umaryland.edu (W.C.) and lzou@som.umaryland.edu (L.Z.)

Abbreviations used in this article: AchE, acetylcholinesterase; BMDM, bone marrow–derived Mϕ; CLP, cecum ligation and puncture; DPBS, Dulbecco's PBS; EV, extracellular vesicle; ex, extracellular; FB, complement factor B; Mϕ, macrophage; miR/miRNA, microRNA; NE, neutrophil; P3C, Pam3cys; PMB, polymyxin B; qRT-PCR, quantitative RT-PCR; WT, wild-type.

This article is distributed under The American Association of Immunologists, Inc., Reuse Terms and Conditions for Author Choice articles.

Copyright © 2018 by The American Association of Immunologists, Inc. 0022-1767/18/$37.50

types of EVs, such as exosomes, apoptotic bodies, and microvesicles (21–23), or bound to proteins such as argonaute-2 (24, 25), all of which reportedly protect them from RNase digestion and carry them to target tissues/cells. Although their plasma concentrations may be modest, emerging data suggest that ex-miRNAs can act on the target cells in a paracrine/endocrine fashion and play an important role in various pathological and inflammatory conditions (26), such as cancer inflammation and metastasis (27), neurodegeneration (28), and pain (29).

We and others have recently demonstrated that host RNAs, including various miRNAs, are released into the blood circulation during sepsis and myocardial ischemia-reperfusion injury in animals (30–32) and patients (33). The host circulating plasma RNA levels are closely associated with sepsis severity in animals (30). Moreover, we have found that ex-RNAs and certain uridine-rich ex-miRNA mimic function as damage-associated molecular patterns and induce both cytokine and complement factor B (FB) production through a specific TLR7- and uridine-dependent mechanism in immune cells, cardiomyocytes, and intact animals (30–32). However, whether these miRNAs are associated with plasma EVs and whether the plasma EVs and their cargo miRNAs play any role in inflammation are unclear.

In the current study, we hypothesized that circulating plasma EVs from septic animals are proinflammatory and that miRNAs associated with septic EVs are responsible for EV-induced inflammatory response. To test this, we isolated EVs from healthy and septic mice, tested their function in vitro and in vivo, and profiled miRNA expression in plasma EVs. Finally, using specific anti-miR inhibitors and TLR knockout mice, we tested the specific role of EV-associated endogenous miRNAs and TLRs in mediating the EV-induced proinflammatory response.

Materials and Methods

Animals

Eight- to twelve-week-old gender- and age-matched mice were used. C57BL/6J wild-type (WT), TLR7$^{-/-}$, and TLR3$^{-/-}$ mice were purchased from The Jackson Laboratory and housed in the University of Maryland School of Medicine animal facility for at least 1 wk before experiments. MyD88$^{-/-}$ mice were generated by Kawai and colleagues (34), and provided water was supplemented with sulfamethoxazole (4 mg/ml) and trimethoprim (0.8 mg/ml). Antibiotics were stopped for at least 2 wk prior to experiments. Trif$^{-/-}$ mice were generated by Yamamoto, et al. (35). All animals were housed in pathogen-free, temperature-controlled, and air conditioned facilities with 12 h/12 h light/dark cycles and fed the same bacteria-free diet. All animal care and procedures were performed according to the protocols approved by the Institutional Animal Care and Use Committee of the University of Maryland School of Medicine and are in compliance with the "Guide for the Care and Use of Laboratory Animals" published by the National Institutes of Health.

Mouse model of polymicrobial sepsis

Polymicrobial sepsis was generated by cecum ligation and puncture (CLP) as described previously (36). In brief, after mice were anesthetized with ketamine (100 mg/kg) and xylazine (10 mg/kg), the cecum was ligated 1.5 cm from the tip, punctured through with an 18-gauge needle, and gently squeezed to take out a small amount of fecal material. The sham-operated mice underwent general anesthesia and laparotomy but without CLP. After surgery, prewarmed saline (0.033 ml/g body weight) was injected s.c., and bupivacaine (3 mg/kg) and buprenorphine (0.1 mg/kg) were administrated s.c. for postoperative pain control.

Isolation and characterization of EVs

EVs were isolated from freshly isolated plasma by differential ultracentrifugation as described previously (37). In brief, 250 μl of plasma was collected and diluted with an equal volume of Ca^{2+}/Mg^{2+}–free Dulbecco's PBS (DPBS) and then centrifuged at 2000 × *g* at 4°C for 30 min to remove cell debris and protein aggregates. Supernatants were transferred to a new Eppendorf tube and centrifuged at 12,000 × *g* at 4°C for 30 min. Subsequently, supernatants were transferred to a new ultracentrifuge tube and diluted with 4 ml of Ca^{2+}/Mg^{2+}–free DPBS and then centrifuged at 120,000 × *g* (MLS-50 Rotor; Beckman Coulter) at 4°C for 120 min. EV pellets were resuspended in 100 μl of cold Ca^{2+}/Mg^{2+}–free DPBS, and EVs were quantified using a nanotracking system (NanoSight LM10; Malvern Panalytical). All EVs used for cell treatment were isolated under sterile conditions. EV proteins were measured with the Bradford method and acetylcholinesterase (AchE) activity was assayed with commercially available kits (Sigma-Aldrich, St. Louis, MO). For electron microscopic imaging, 25 μl of isolated plasma EVs were treated in 2% paraformaldehyde and fixed on a 400-mesh square copper grid with 2% uranyl acetate.

EV miRNA array

RNA isolated from 20 μl of plasma EVs of sham and CLP mice was used to profile miRNAs using a FirePlex miRNA Panel – Immunology V2 as we previously reported (30) (Abcam, Boston, MA). The technology employs a unique posthybridization ligation-based scheme to fluorescently label bound miRNA targets.

EV miRNA detection by quantitative RT-PCR

Total RNA was isolated from 250 μl of plasma-derived EVs using miRNeasy Micro Kit (QIAGEN, Germantown, MD). A spike-in control, *Caenorhabditis elegans* miRNA (cel-miR-39), was added prior to the RNA extraction. RNA pellets were resuspended in 14 μl of RNase-free water and quantified using Quant-iT RNA Assay Kit (Invitrogen, Waltham, MA) as reported previously (30, 32). Twelve microliters of RNA solution were used for reverse transcription, according to the protocol of miScript RT Kit (QIAGEN). miRNA expression was quantified using a miScript SYBR Green PCR Kit (QIAGEN). Relative expression was calculated using the comparative cycle threshold (Ct) method ($2^{-\triangle\triangle Ct}$) normalized to spike-in *C. elegans* miRNA (cel-miR-39) and expressed as the fold change in CLP EVs over sham EVs.

Isolation and culture of bone marrow–derived macrophages

Bone marrow cells were harvested from mouse tibias and femurs, cultured, and differentiated into macrophages (Mϕs) in the presence of M-CSF (10 ng/ml) as described previously with minor modifications (32). In brief, bone marrow cells were cultured in RPMI 1640 culture medium (Thermo Fisher Scientific) with 10% FBS (Thermo Fisher Scientific), 5% horse serum (Thermo Fisher Scientific), and penicillin (100 U/ml)/streptomycin (100 μg/ml) (Thermo Fisher Scientific) and seeded in a 96-well plate (2×10^5 cells per well) in a CO_2 incubator at 37°C. Three days later, culture media were changed, and Mϕs were ready for experiments at day 4.

Cell treatment

Bone marrow–derived Mϕs (BMDM) were incubated in serum-free culture medium containing 0.05% BSA for 1 h before treatment with EVs (20 μg/ml), poly(I:C) (10 μg/ml; Enzo Life Sciences, Farmingdale, NY), R837 (1μg/ml; InvivoGen, San Diego, CA), or Pam3Cys (P3C; 1μg/ml; Enzo Life Sciences) for overnight. To eliminate possible effects of potential endotoxin contamination, EVs (20 μg/ml) were incubated with 10 μg/ml polymyxin B (PMB) (Sigma-Aldrich) at 4°C for 1 h prior to the treatment to the cells.

For nuclease and anti-miR treatment, RNase (Sigma-Aldrich), DNase (Thermo Fisher Scientific, Waltham, MA), Benzonase (Millipore, Billerica, MA), and miRNA inhibitor (miRCURY LNA Power microRNA Inhibitors; Exiqon) were preincubated with sham or CLP–EVs, splenic RNA (50 μg/ml), thymic DNA (10 μg/ml; Thermo Fisher Scientific), and miR-146a mimics (50 nM; Integrated DNA Technologies, Skokie, IL) at room temperature for 1 h before being applied to cell cultures. Lipofectamine 3000 (Thermo Fisher Scientific) was used to complex the RNA, DNA, and miRNA mimics according to the manufacturer's protocol.

Cytokine assays

Medium MIP-2, IL-6, TNF-α, and IL-1β were detected using ELISA kits (R&D Systems, Minneapolis, MN), as described previously (32).

Western blotting

EV proteins were lysed with SDS sample buffer and separated in 4–12% gradient SDS-PAGE and immunoblotted with Abs (1:1000) against CD81 (Cell Signaling Technology, Danvers, MA). Western blotting bands were visualized using Luminata Forte Western HRP substrate (Millipore) and imaged in a ChemiDoc system (Bio-Rad Laboratories, Hercules, CA). The band intensity was quantified using National Institutes of Health Image J.

In vivo EV administration

After shaving the fur and disinfecting the abdominal skin, mice were administered sham or CLP EVs (300 μg/mouse) through i.p. injection using

31gauge insulin syringes. An adhesive 3M Tegaderm film was applied to cover the injection site to prevent infection. Eighteen hours later, the peritoneal lavage was harvested as described previously (31). Briefly, 5 ml of saline was injected into the peritoneal space and mixed thoroughly by gentle massage of the abdomen. The peritoneal lavage was collected and centrifuged. The cell pellets were suspended in DPBS, and total peritoneal cells were counted. A total of 4×10^5 cells were incubated with specific Alexa Fluor 647 rat anti-mouse F4/80 (eBioscience, San Diego, CA) and Percp-cy 5.5 rat anti-mouse Ly-6G (BD Biosciences, San Jose, CA) at 4°C for 15 min protected from light. After washing with 4 ml of cold DPBS, cell pellets were suspended in DPBS with 5% FBS and analyzed in a BD FACSCanto II flow cytometer (BD Biosciences) as described previously (32).

Statistical analysis

Statistical analysis was performed using GraphPad Prism 5 software (GraphPad, La Jolla, CA). The distributions of the continuous variables were expressed as mean ± SEM. One-way ANOVA with Tukey post hoc analysis or two-way ANOVA with Bonferroni post hoc analysis was applied to test the effects of anti-miR. The statistical significance of the difference between groups was measured by two-tailed unpaired Student *t* test, and a p value < 0.05 was considered significant.

Results

Characterization of plasma EVs in sham and septic mice

Mice were subjected to sham or CLP procedures. Twenty-four hours later, mice were anesthetized, blood was collected, and plasma was prepared for EV isolation. Fig. 1A shows a representative electron microscopy image of EVs isolated from a septic mouse. Nanotracking analysis revealed that the plasma EV particles had size distribution between 50 and 300 nm (Fig. 1B). Compared with sham mice, plasma EVs in CLP mice had slightly smaller size on average (medium size: 157 ± 2 versus 191 ± 6 nm, $p < 0.001$) (Fig. 1B), but were present in higher numbers [$(1.60 \pm 0.14) \times 10^{10}$ versus $(0.93 \pm 0.14) \times 10^{10}$/ml plasma, $p < 0.003$] (Fig. 1C). When compared with EVs from sham animals, EVs of CLP animals had similar amounts of protein contents (Fig. 1D) but possessed higher AchE activity (Fig. 1E) and CD81 expression (Fig. 1F).

Plasma EVs of CLP mice induce marked cytokine production

To determine whether plasma EVs were biologically active, we treated BMDM with 20 μg/ml of EVs isolated from both sham and CLP mice and assayed the culture medium for cytokines 20 h later. As illustrated in Fig. 2A, the medium levels of MIP-2, IL-6, IL-1β, and TNF-α were a marked increase in the CLP EV–treated cells compared with those treated with sham EVs. The CLP EV–induced MIP-2 and IL-6 responses were dose-dependent, whereas the sham EVs did not induce cytokine production within the same dose ranges (10–100 μg/ml) (Fig. 2B). To exclude the possibility that endotoxin was associated with the CLP plasma EVs and contributed to the observed cytokine responses, we pretreated the plasma EVs with PMB, a potent endotoxin (LPS) inhibitor. As shown in Fig. 2C, CLP EVs, P3C (a TLR2 ligand), and LPS (endotoxin, a TLR4 ligand) all induced a robust MIP-2 response. Although PMB completely abolished the effect of LPS, it had no effect on the CLP EV– or P3C-induced cytokine productions, suggesting that endotoxin played no role in the CLP EV–induced cytokine production in BMDM.

EV miRNA analysis

Plasma EVs are known as carriers for circulating miRNAs. We have reported previously that plasma host RNAs and miRNAs are elevated following polymicrobial infection and that plasma RNA levels are closely correlated with sepsis severity (30). To explore the role of EV-associated miRNAs in CLP EV–mediated cytokine responses, we first examined the amount of RNA associated with plasma EVs in sham and CLP mice. As shown in Fig. 3A, there was a significant increase in the amount of RNA associated with CLP EVs as compared with that of sham EVs (221.7 ± 39.0 versus 56.7 ± 7.2 ng/ml) isolated from the same plasma volume. We next probed 65 miRNAs reportedly related to immunologic functions using a miRNA array and found eight miRNAs that were increased >1.5-fold in CLP EVs compared with sham EVs that also displayed fluorescence counts >100 (Fig. 3B–D), including miR-126-3p, miR-122-5p, miR-146a-5p, miR-145-5p, miR-26a-5p, miR-150-5p, miR-22-3p, and miR-181a-5p. The complete miRNA array data (accession no. GSE116829) can be accessed at https://www.ncbi.nlm.nih.gov/geo/query/acc.cgi?acc=GSE116829. Importantly, out of the eight miRNAs, all, with exception of miR-181a-5p, were validated by quantitative RT-PCR (qRT-PCR) (Fig. 3E). Of note, miR-34a-5p, which was significantly increased in septic plasma in our previous report (30), was found by qRT-PCR to be significantly upregulated in the CLP EVs (Fig. 3E), despite its low expression level in the

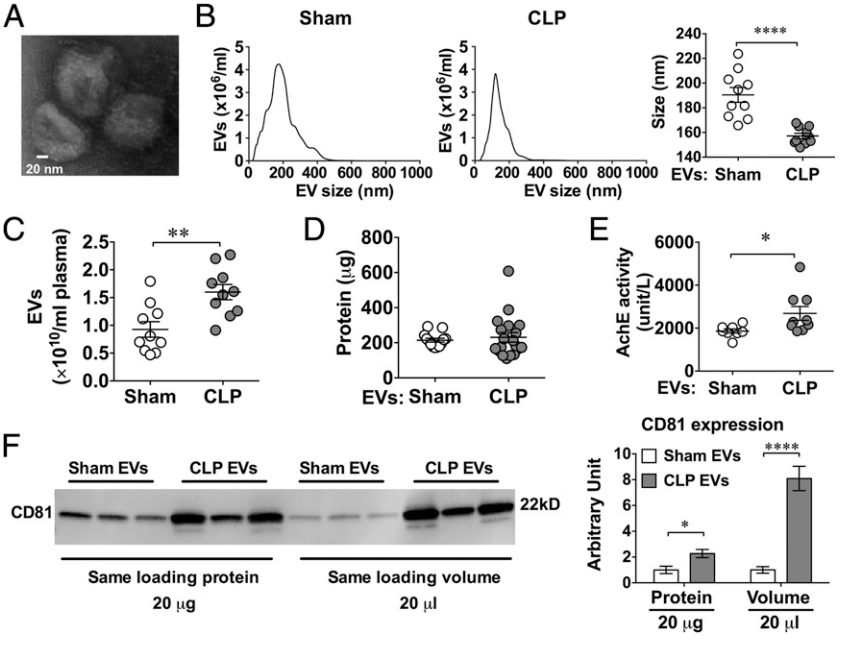

FIGURE 1. Characterization of EVs isolated from the plasma of CLP and sham mice. (**A**) A representative electron microscopic image of septic plasma EVs. Mice were subjected to sham or CLP surgery. EVs were purified from plasma 24 h after surgery. Scale bar, 20 nm. (**B**) Plasma EV size distribution as measured by NanoSight. (**C**) EV particle numbers as quantified by NanoSight. (**D**) Protein quantification of EVs derived from 250 μl of plasma by Bradford assay. (**E**) EV AchE activity. (**F**) CD81 protein expression in EVs was quantified by Western blot, loading with the same amount of EV protein (20 μg) or the same volume of EV solution (20 μl) ($n = 3$). *$p < 0.05$, **$p < 0.01$, ****$p < 0.0001$.

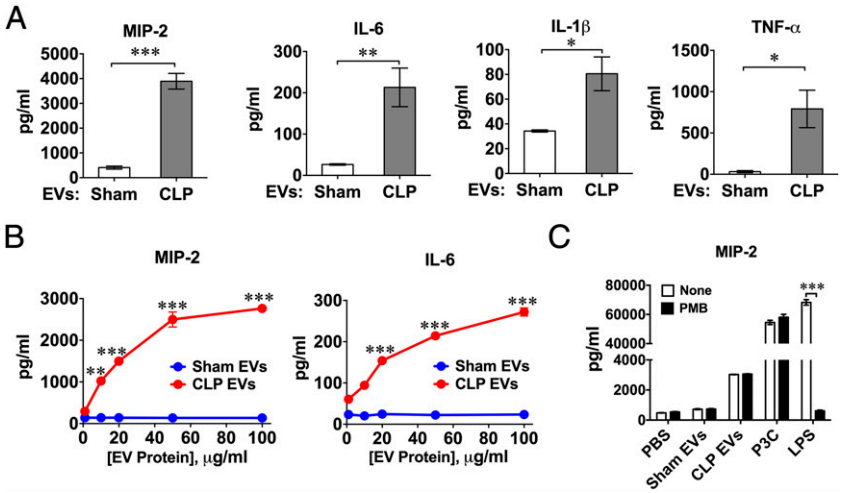

FIGURE 2. Plasma EVs from septic mice induce cytokine production in BMDM. BMDM were treated with plasma EVs isolated from mice 24 h after sham or CLP procedure. The culture media were collected 16 h later for cytokine assays. (**A**) Medium cytokines (MIP-2, IL-6, IL-1β, TNF-α) were measured by ELISA. The concentration of EVs was 20 μg/ml protein in both sham and CLP group (n = 3–17). (**B**) Dose-dependency of EV-induced cytokine (MIP-2 and IL-6) production. Each bar represents triplicate samples with each experiment repeated twice. $^{**}p < 0.01$, $^{***}p < 0.001$, versus sham EVs. (**C**) Effect of PMB on MIP-2 production in BMDM. EVs (20 μg/ml), P3C (1 μg/ml), or LPS (10 ng/ml) were pretreated with 10 μg/ml of PMB for 1 h at 4°C before being applied to BMDM cultures. Each bar represents triplicate samples with each experiment repeated three times. $^{*}p < 0.05$, $^{**}p < 0.01$, $^{***}p < 0.001$.

plasma EVs as determined by the array (mean fluorescence intensity < 100, CLP/sham = 1.54).

Anti-miRs attenuate CLP EV–induced cytokine production

Because miR-122, miR-146a, and miR-34a are upregulated in septic plasma and EVs and possess proinflammatory properties, such as production of cytokines and FB and activation of cellular MAPK and NF-κB (30, 32), we decided to test the contribution of these specific cargo miRNAs to CLP EV–induced cytokine production. To achieve this, we pretreated EVs for 1 h with anti–miR-34a, anti–miR-122, or anti–miR-146a at a concentration of 100 nM. As shown in Fig. 4A, each of these anti-miR inhibitors or the

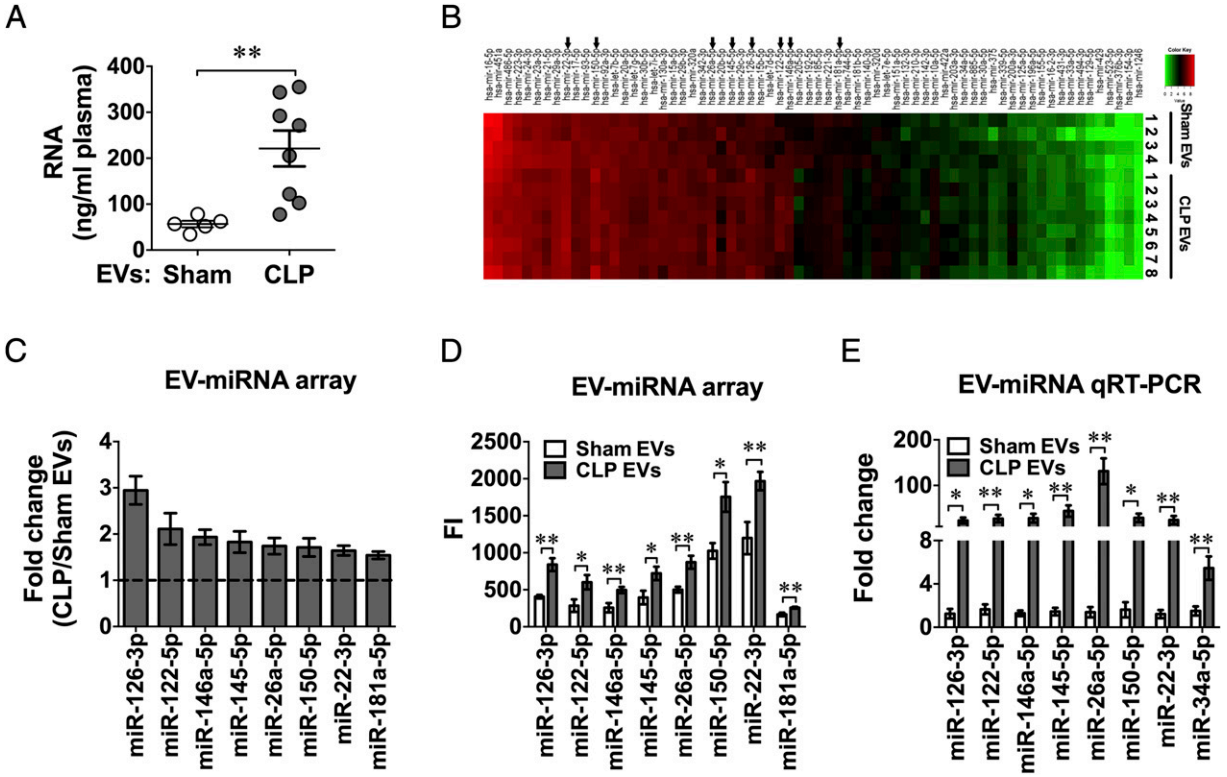

FIGURE 3. Plasma EV RNA qualification and miRNA profiling. Total RNA was extracted from EVs isolated from 250 μl of plasma 24 h after sham or CLP surgery. (**A**) EV RNA quantitation. (**B**) Heat map of EV miRNA microarray. The fluorescence intensity of 65 miRNAs was illustrated from high (red) to low (green). (**C**) Differential expression of plasma EV miRNAs between CLP and sham plasma expressed as fold change (CLP/sham) as determined by miRNA array (n = 4–8). (**D**) Mean fluorescent intensity (FI) of EV miRNAs as measured by miRNA array from sham and CLP mice [n = 5 in sham group, except miR-122 (n = 4), n = 8 in CLP group]. (**E**) qRT-PCR analysis of plasma EV miRNAs. The EV miRNAs identified by miRNA arrays were analyzed using qRT-PCR in a separate set of EVs (n = 4–18). $^{*}p < 0.05$, $^{**}p < 0.01$.

combination of all three anti-miRNAs reduced CLP EV–induced MIP-2 production by 40–60%. To determine the robustness of the EV-associated effects, we pretreated miR-146a (50 nM), mouse splenic RNA (50 μg/ml), mouse thymic DNA (10 μg/ml), and sham/CLP EVs with RNase (10 μg/ml), DNase (50 U/ml), or Benzonase (50 U/ml) before applying them to cell cultures. As shown in Fig. 4B, 4C, whereas RNase or DNase treatment abolished the MIP-2 production induced by miR-146a mimic, splenic RNA, or thymic DNA, respectively, these nuclease (DNase, RNase, or Benzonase) treatments had no effect on the CLP EV–induced MIP-2 production (Fig. 4B, 4C). Overall, these results suggest that CLP EVs may induce cytokine production via delivery of miRNAs that are associated with the EVs in such a way (e.g., encapsulation) that they are protected from nuclease degradation.

CLP EVs induce cytokine response via a TLR7-MyD88–dependent mechanism in Mϕs

We have previously reported that ex-RNAs and certain uridine-rich miRNA mimics induce cytokine and FB production through TLR7 (30–32). Hence, we hypothesized that CLP EVs induce cytokine response via a similar mechanism. We isolated BMDM from WT, TLR7$^{-/-}$, TLR3$^{-/-}$, MyD88$^{-/-}$, and Trif$^{-/-}$ mice and treated them with sham EVs and CLP EVs. As shown in Fig. 5A, 5B, CLP EVs induced robust production of MIP-2 and IL-6 in WT BMDM. Although this effect largely remained the same in TLR3$^{-/-}$ cells, it was markedly attenuated in TLR7$^{-/-}$ cells. We also included a few TLR ligands (TLR3–poly(I:C), TLR2–P3C, TLR7–R837) in these experiments as controls. As anticipated, TLR7$^{-/-}$ cells failed to respond to R837, whereas TLR3$^{-/-}$ cells did not respond to poly(I:C). In contrast, both TLR3$^{-/-}$ and TLR7$^{-/-}$ cells responded normally to P3C. Importantly, deficiency of MyD88, the key adaptor of several TLRs, including TLR7 and TLR2, completely inhibited CLP EV– and P3C-induced cytokine production but, as anticipated, had no effect on the poly(I:C)-induced effect (Fig. 5B). In contrast, Trif-deficiency, although blocking the effect of poly(I:C), had no impact on the effect of the EVs or P3C. Taken together, these data clearly suggest that CLP EVs induce both MIP-2 and IL-6 production through a TLR7-MyD88–dependent mechanism in Mϕs.

CLP EVs induce FB and C3 complement factor production in Mϕs

Complement components such as C3, C4, C5, and FB are important parts of the host innate immune system and play important roles in sepsis pathogenesis (38). To determine whether plasma EVs have any effect on complement production, we treated BMDM with 20 μg/ml of EVs and tested for FB and C3, C4, and C5 expression. As shown in Fig. 6, 6 h after treatments, CLP EVs induced a robust increase (>30-fold) in gene expression of FB and C3 but not C4 or C5 as compared with sham EVs.

CLP EVs attract peritoneal leukocyte migration in vivo

To examine whether CLP EVs also induce inflammation in vivo, we injected saline, sham EVs, or CLP EVs into the mouse peritoneal space (300 μg/mouse). The peritoneal cells were harvested and counted 18 h later for flow cytometry analysis. As shown in Fig. 7A, the peritoneal cells were gated for Mϕs (F4/80^{high}) and neutrophils (NE; Ly-6G^{+}). As illustrated in Fig. 7B and 7C, compared with saline or sham EVs, CLP EVs induced a significant reduction in the number of peritoneal Mϕs and a marked increase in the number of peritoneal NEs. Of note, whereas sham EVs had no effect on the peritoneal Mϕ numbers, they induced a modest increase in the peritoneal NEs as compared with saline [$(0.55 \pm 0.09) \times 10^5$ versus $(0.04 \pm 0.02) \times 10^5$, $n = 6$]. Surprisingly, systemic deletion of TLR7 had no significant effect on CLP EV–induced Mϕ reduction or NE increase in the peritoneal space (Fig. 7D, 7E). In contrast, systemic deletion of MyD88, a key adaptor for multiple TLRs, including TLR2, TLR4, TLR7/8, and TLR9, significantly reduced both sham EV– and CLP EV–induced NE recruitment (Fig. 7F, 7G).

Discussion

We tested our hypothesis that plasma EVs from septic animals are highly proinflammatory and that EV-associated miRNAs are

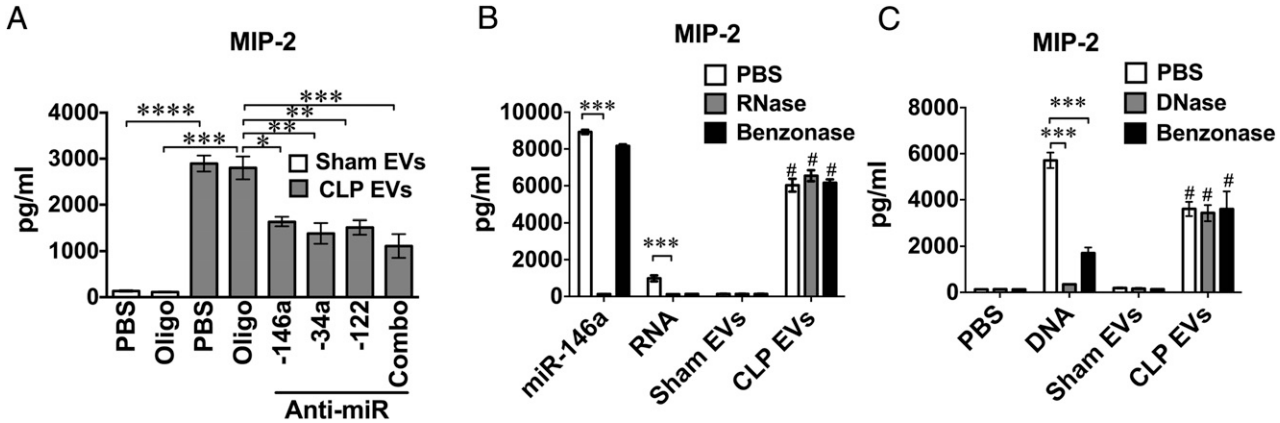

FIGURE 4. Anti-miRs but not nucleases partially reduce CLP EV–induced cytokine production. (**A**) Anti-miR treatment of EVs partially attenuated the CLP EV–induced cytokine production. Prior to applying to BMDM cultures, sham EVs were treated with PBS or control oligonucleotide (Oligo) at 300 nM. CLP EVs (20 μg/ml) were incubated with PBS, control Oligos (300 nM), single anti-miR (anti–miR-146a, anti–miR-34a, and anti–mir-122, at 100 nM), or anti-miR combination at 300 nM, including anti–miR-146a, anti–miR-34a, and anti–miR-122 for 1 h. Cell culture media were collected 16 h after treatment and assayed for MIP-2 production using ELISA. Each bar represents triplicate samples with each experiment repeated twice. *$p < 0.05$, **$p < 0.01$, ***$p < 0.001$, ****$p < 0.001$. (**B**) RNase or Benzonase had no impact on CLP EV–induced MIP-2 production. miR-146a mimic (50 nM), splenic RNA (50 μg/ml), sham EVs (20 μg/ml), and CLP EVs (20 μg/ml), were incubated with PBS, RNase (10 μg/ml), or Benzonase (50 U/ml) for 1 h at room temperature before being applied to BMDM cultures. Sixteen hours later, media were collected for MIP-2 ELISA. Each bar represents triplicate samples with each experiment repeated twice. ***$p < 0.001$, #$p < 0.0001$, versus sham EVs. (**C**) DNase or Benzonase had no impact on CLP EV–induced MIP-2 production. miRNA-146a mimics (50 nM), thymic DNA (10 μg/ml), sham EVs (20 μg/ml), and CLP EVs (20 μg/ml) were incubated with PBS, DNase (50 U/ml), or Benzonase (50 U/ml) for 1 h at room temperature before being applied to BMDM. Sixteen hours later, medium MIP-2 was analyzed by ELISA. Each bar represents triplicate samples with each experiment repeated twice. ***$p < 0.001$, #$p < 0.0001$, versus sham EVs.

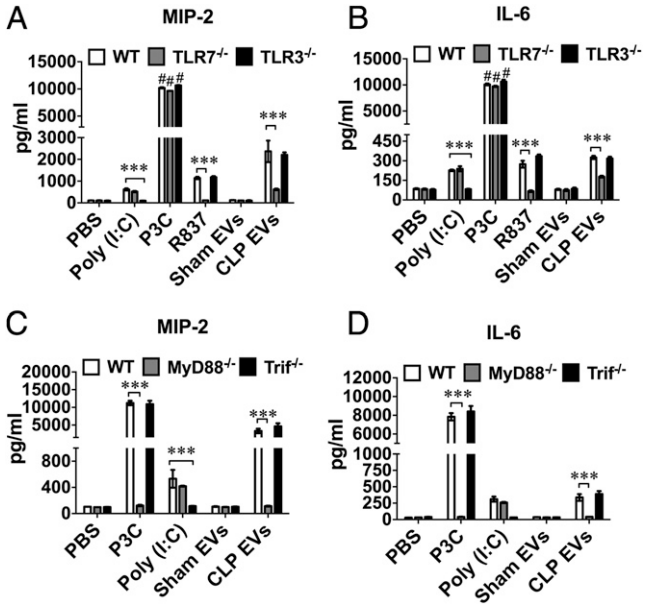

FIGURE 5. Plasma EVs from septic mice induce cytokine production through TLR7-MyD88 signaling. BMDM were isolated from WT and genetically modified mice ($TLR7^{-/-}$, $TLR3^{-/-}$, $MyD88^{-/-}$, $Trif^{-/-}$) and treated with sham EVs (20 μg/ml), CLP EVs (20 μg/ml), P3C (TLR2 ligand, 1 μg/ml), poly(I:C) (TLR3 ligands, 10 μg/ml), or R837 (TLR7 ligand, 0.25 μg/ml). Sixteen hours after the treatment, the culture media were collected and cytokines (MIP-2, IL-6) were measured by ELISA. (**A** and **B**) TLR7 but not TLR3 signaling contributed to CLP EV–induced cytokine production. (**C** and **D**) MyD88- but not Trif-deficiency abolished CLP EV–mediated MIP-2 and IL-6 production. Each bar represents triplicate samples with each experiment repeated twice. $***p < 0.001$, $\#p < 0.0001$, versus PBS group.

responsible for the innate immune response. We made a few novel observations. First, we found that septic mice had increased numbers of plasma EVs with more abundant RNA compared with sham animals. miRNA array analysis revealed a group of eight miRNAs significantly upregulated in the septic plasma EVs. Second, plasma EVs isolated from septic mice but not those from sham mice induced robust production of MIP-2, IL-6, IL-β, TNF-α, and FB. Pretreatment of plasma EVs with miRNA inhibitors against miR-146a, miR-122, miR-34a, or a combination led to a 40–60% reduction of the cytokine production induced by CLP EVs. The loss-of-function studies indicated that EV-induced cytokine production was in part dependent on TLR7–MyD88 signaling but independent of TLR3 and resistant to nuclease digestion. Finally, in vivo, peritoneal injection of CLP EVs induced significant recruitment of NEs and reduction of residential Mϕs in the peritoneal cavity. Surprisingly, such effects of plasma EVs remained intact in $TLR7^{-/-}$ mice but were abolished in $MyD88^{-/-}$ animals.

Circulating EVs have been reportedly associated with critical illnesses such as sepsis and various organ injuries (39). Both human and animal studies have suggested a possible role of plasma EVs in sepsis. For example, an early study by Janiszewski and coworkers (40) found that EVs isolated from septic patients possess NADPH oxidase activity and induce reactive oxygen species production and apoptosis in endothelial cell cultures. The same group also reported that platelet-derived EVs from septic shock patients induce myocardial dysfunction (41). Moreover, an animal study by Fan and coworkers (42) demonstrated that pharmacological blockade of EV generation attenuated cytokine production in LPS-treated Mϕs in vitro and mice in vivo as well as endotoxin-induced cardiac dysfunction. Expanding on these observations, we found that plasma EVs from polymicrobial septic mice but not healthy sham mice possess the remarkable ability of inducing proinflammatory cytokine production in Mϕs. The effect appears to be dose-dependent and is unlikely to be related to endotoxin. These data establish an important role for circulating plasma EVs as a potential proinflammatory mediator in polymicrobial sepsis.

EVs have emerged as both critical mediators of intercellular communication in health and diseases as well as potential therapeutic vectors. EVs harbor a wide variety of miRNAs and can deliver ex-RNA/miRNAs to target cells nearby or at distance (43–45). To identify specific ex-miRNAs loaded in the plasma EVs, we tested the differential expression of 65 miRNAs involved in the immune function between sham and CLP EVs. Using miRNA arrays, we found that eight miRNAs, including miR-126-3p, miR-122-5p, miR-146a-5p, miR-145-5p, miR-26a-5p, miR-150-5p, miR-22-3p, and miR-181a-5p, were upregulated in the circulating EVs of CLP mice compared with those of sham mice. These data are consistent with our previous study, in which some of these miRNAs (i.e., miR-122-5p, miR-34a-5p, miR-145a-5p, and miR-146a-5p) were expressed at higher levels in the plasma of CLP mice, and a few uridine-rich miRNA mimics (miR-34a-5p, miR-145a-5p, and miR-146a-5p) exhibited a remarkable ability to induce cytokine (32) and FB (30) production.

To determine whether ex-miRNAs loaded in the plasma EVs are functionally active and responsible for the cytokine production in Mϕs treated with the CLP EVs, we employed three synthetic miRNA inhibitors to specifically block EV-associated miRNAs (i.e., miR-122, miR-146a, and miR-34a). We chose these three miRNAs to block for two reasons: 1) they induce a robust production of both cytokines (32) and FB (30) in Mϕs, and 2) they are upregulated in the plasma (30) and the plasma EVs (Fig. 3) of septic mice compared with that of sham mice. We found that these miRNA inhibitors but not control oligonucleotides partially inhibited CLP EV–elicited cytokine production. These data support the notion that the endogenous miRNAs play a direct role in CLP EV–induced cytokine production. The partial inhibition suggests a possibility that other EV-associated miRNAs or cargo components,

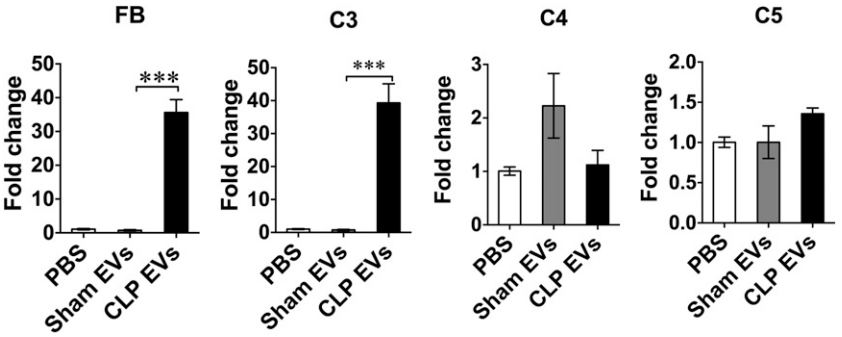

FIGURE 6. CLP EVs induce FB and C3 production in Mϕs. BMDM were treated with PBS, sham EVs (20 μg/ml), or CLP EVs (20 μg/ml) for 6 h and extracted for total RNA. Transcripts for FB, C3, C4, and C5 in each group were analyzed by qRT-PCR and normalized to GAPDH. Each bar represents triplicate samples with each experiment repeated twice. $***p < 0.001$.

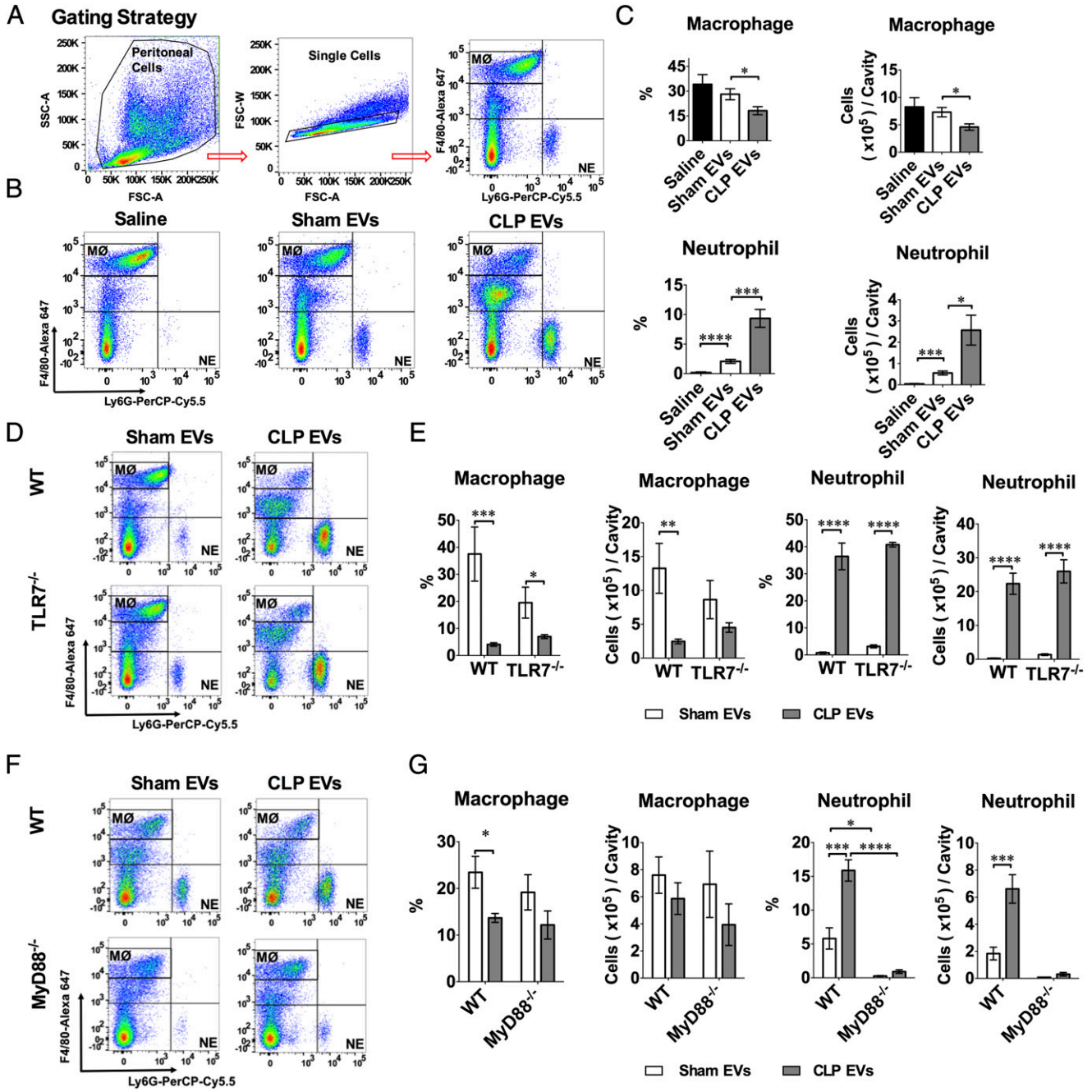

FIGURE 7. CLP EVs promote peritoneal leukocyte recruitment in vivo. WT, TLR7$^{-/-}$, and MyD88$^{-/-}$ male mice were administered i.p. saline, 300 μg of sham EVs, or CLP EVs. Twenty hours later, the peritoneal lavage was harvested, and the peritoneal cells were analyzed with flow cytometry. (**A**) Gating strategy for flow cytometry. F4/80^{high}–Alexa Fluro 647 were determined as resident Mϕ and Ly-6G^{+}-Percp-Cy5.5 were determined as NE. (**B**) Representative flow cytometry of gated F4/80^{high} and Ly-6G^{+} in peritoneal cells of WT mice i.p. injected with saline, sham EVs, or CLP EVs. (**C**) CLP EVs reduce resident Mϕs and promote NEmigration into the peritoneal cavity as compared with sham EVs ($n = 6$). (**D** and **E**) TLR7 deficiency has no impact on CLP EV–induced Mϕ reduction and NE increase in the peritoneal cavity ($n = 5$–6). (**F** and **G**) MyD88-deficient mice had reduced NE migration to the peritoneal cavity after sham EV and CLP EV injection as compared with WT mice ($n = 3$–4). *$p < 0.05$, **$p < 0.01$, ***$p < 0.001$, ****$p < 0.0001$.

such as noncoding RNAs, DNAs, lipids, or proteins, may also play a role. Finally, we found that RNase or DNase treatments had no impact on CLP EV–induced MIP-2 production, whereas the same treatments abolished the effect of splenic RNA and thymic DNA, respectively. These observations may indicate a protective effect of plasma EVs for their cargo RNA/DNA against the digestive nucleases, a well-documented function of circulating EVs (21–23). Thus, these data establish a pivotal role of EV-associated miRNAs in the proinflammatory effect of circulating plasma EVs in polymicrobial sepsis.

One important finding of the current study is the discovery of the important role of TLR7–MyD88 signaling in the CLP EV–induced cytokine production in Mϕs. Using various knockout mouse models, we demonstrate the necessity of TLR7 and MyD88 in EV-induced cytokine production. The data are consistent with our previous findings that certain uridine-rich miRNA mimics act through the TLR7–MyD88 axis to activate innate immune function in vivo and in vitro (30, 32). Supporting this notion are our confocal imaging analyses illustrating the partial colocalization of miRNAs, TLR7, and endosomes in both Mϕ and cardiomyocytes (32) and the

physical association of miR-146a and TLR7 as demonstrated by co-immunoprecipitation assay (S. Wang and W. Chao, unpublished observations). It is possible that circulating EVs function as miRNA carriers and deliver multiple miRNAs to target cells that activate endosomal TLR7–MyD88 signaling.

We found that plasma EVs isolated from septic mice were capable of inducing marked NE migration to and reduction of resident Mϕs in the peritoneal cavity when injected i.p. These in vivo data clearly confirm the proinflammatory property of these plasma EVs. To our surprise, unlike the cytokine responses in Mϕs, TLR7 deficiency has no impact on CLP EV–induced leukocyte migration. These data suggest that these in vivo effects are not exclusively mediated through TLR7 or even miRNAs, and other pathways or mediators may be responsible. In contrast, MyD88 deficiency markedly attenuated peritoneal NE migration induced by both sham and CLP EVs, suggesting that EV-elicited NE recruitment is dependent on MyD88. We have reported that MyD88 signaling plays an important role in NE migration by regulating peritoneal chemokine production and NE CXCR2 expression in a chemical peritonitis model (46). Whether or not these mechanisms play a role in the plasma EV–induced NE migration remains to be investigated.

In summary, we found, in a mouse model of polymicrobial sepsis, that circulating plasma EVs are highly proinflammatory, inducing dose-dependent cytokine production, FB synthesis, and NE migration. miRNA array analysis identified multiple proinflammatory ex-miRNAs that are in part responsible for the observed EV-elicited cytokine responses. Importantly, these proinflammatory responses appear to be mediated via TLR7- and/or MyD88-dependent mechanisms. Together, our data have identified plasma EVs and their cargo miRNAs as a potential proinflammatory mediators during polymicrobial sepsis.

Acknowledgments

We thank Dr. Xiaoxuan Fan (Flow Cytometry Core, University of Maryland School of Medicine) for technical support.

Disclosures

The authors have no financial conflicts of interest.

References

1. Singer, M., C. S. Deutschman, C. W. Seymour, M. Shankar-Hari, D. Annane, M. Bauer, R. Bellomo, G. R. Bernard, J. D. Chiche, C. M. Coopersmith, et al. 2016. The third international consensus definitions for sepsis and septic shock (sepsis-3). *JAMA* 315: 801–810.
2. Angus, D. C., W. T. Linde-Zwirble, J. Lidicker, G. Clermont, J. Carcillo, and M. R. Pinsky. 2001. Epidemiology of severe sepsis in the United States: analysis of incidence, outcome, and associated costs of care. *Crit. Care Med.* 29: 1303–1310.
3. Rhee, C., R. Dantes, L. Epstein, D. J. Murphy, C. W. Seymour, T. J. Iwashyna, S. S. Kadri, D. C. Angus, R. L. Danner, A. E. Fiore, et al; CDC Prevention Epicenter Program. 2017. Incidence and trends of sepsis in US hospitals using clinical vs claims data, 2009-2014. *JAMA* 318: 1241–1249.
4. EL Andaloussi, S., I. Mäger, X. O. Breakefield, and M. J. Wood. 2013. Extracellular vesicles: biology and emerging therapeutic opportunities. *Nat. Rev. Drug Discov.* 12: 347–357.
5. Dalvi, P., B. Sun, N. Tang, and L. Pulliam. 2017. Immune activated monocyte exosomes alter microRNAs in brain endothelial cells and initiate an inflammatory response through the TLR4/MyD88 pathway. *Sci. Rep.* 7: 9954.
6. Zempleni, J., A. Aguilar-Lozano, M. Sadri, S. Sukreet, S. Manca, D. Wu, F. Zhou, and E. Mutai. 2017. Biological activities of extracellular vesicles and their cargos from bovine and human milk in humans and implications for infants. *J. Nutr.* 147: 3–10.
7. Zhao, Y., H. Wang, M. Lu, X. Qiao, B. Sun, W. Zhang, and D. Xue. 2016. Pancreatic acinar cells employ miRNAs as mediators of intercellular communication to participate in the regulation of pancreatitis-associated macrophage activation. *Mediators Inflamm.* 2016: 6340457.
8. Mastronardi, M. L., H. A. Mostefai, F. Meziani, M. C. Martínez, P. Asfar, and R. Andriantsitohaina. 2011. Circulating microparticles from septic shock patients exert differential tissue expression of enzymes related to inflammation and oxidative stress. *Crit. Care Med.* 39: 1739–1748.
9. Vasudevan, S., Y. Tong, and J. A. Steitz. 2007. Switching from repression to activation: microRNAs can up-regulate translation. *Science* 318: 1931–1934.
10. Ling, H., M. Fabbri, and G. A. Calin. 2013. MicroRNAs and other non-coding RNAs as targets for anticancer drug development. *Nat. Rev. Drug Discov.* 12: 847–865.
11. van Rooij, E., and E. N. Olson. 2012. MicroRNA therapeutics for cardiovascular disease: opportunities and obstacles. *Nat. Rev. Drug Discov.* 11: 860–872.
12. Small, E. M., R. J. Frost, and E. N. Olson. 2010. MicroRNAs add a new dimension to cardiovascular disease. *Circulation* 121: 1022–1032.
13. van Rooij, E. 2012. Introduction to the series on microRNAs in the cardiovascular system. *Circ. Res.* 110: 481–482.
14. Chim, S. S., T. K. Shing, E. C. Hung, T. Y. Leung, T. K. Lau, R. W. Chiu, and Y. M. Lo. 2008. Detection and characterization of placental microRNAs in maternal plasma. *Clin. Chem.* 54: 482–490.
15. Lawrie, C. H., S. Gal, H. M. Dunlop, B. Pushkaran, A. P. Liggins, K. Pulford, A. H. Banham, F. Pezzella, J. Boultwood, J. S. Wainscoat, et al. 2008. Detection of elevated levels of tumour-associated microRNAs in serum of patients with diffuse large B-cell lymphoma. *Br. J. Haematol.* 141: 672–675.
16. Mitchell, P. S., R. K. Parkin, E. M. Kroh, B. R. Fritz, S. K. Wyman, E. L. Pogosova-Agadjanyan, A. Peterson, J. Noteboom, K. C. O'Briant, A. Allen, et al. 2008. Circulating microRNAs as stable blood-based markers for cancer detection. *Proc. Natl. Acad. Sci. USA* 105: 10513–10518.
17. Chen, X., Y. Ba, L. Ma, X. Cai, Y. Yin, K. Wang, J. Guo, Y. Zhang, J. Chen, X. Guo, et al. 2008. Characterization of microRNAs in serum: a novel class of biomarkers for diagnosis of cancer and other diseases. *Cell Res.* 18: 997–1006.
18. Hanke, M., K. Hoefig, H. Merz, A. C. Feller, I. Kausch, D. Jocham, J. M. Warnecke, and G. Sczakiel. 2010. A robust methodology to study urine microRNA as tumor marker: microRNA-126 and microRNA-182 are related to urinary bladder cancer. *Urol. Oncol.* 28: 655–661.
19. Kosaka, N., H. Izumi, K. Sekine, and T. Ochiya. 2010. microRNA as a new immune-regulatory agent in breast milk. *Silence* 1: 7.
20. Weber, J. A., D. H. Baxter, S. Zhang, D. Y. Huang, K. H. Huang, M. J. Lee, D. J. Galas, and K. Wang. 2010. The microRNA spectrum in 12 body fluids. *Clin. Chem.* 56: 1733–1741.
21. Valadi, H., K. Ekström, A. Bossios, M. Sjöstrand, J. J. Lee, and J. O. Lötvall. 2007. Exosome-mediated transfer of mRNAs and microRNAs is a novel mechanism of genetic exchange between cells. *Nat. Cell Biol.* 9: 654–659.
22. Hunter, M. P., N. Ismail, X. Zhang, B. D. Aguda, E. J. Lee, L. Yu, T. Xiao, J. Schafer, M. L. Lee, T. D. Schmittgen, et al. 2008. Detection of microRNA expression in human peripheral blood microvesicles. [Published erratum appears in 2010 *PLoS One* 5] *PLoS One* 3: e3694.
23. Zernecke, A., K. Bidzhekov, H. Noels, E. Shagdarsuren, L. Gan, B. Denecke, M. Hristov, T. Köppel, M. N. Jahantigh, E. Lutgens, et al. 2009. Delivery of microRNA-126 by apoptotic bodies induces CXCL12-dependent vascular protection. *Sci. Signal.* 2: ra81.
24. Turchinovich, A., L. Weiz, A. Langheinz, and B. Burwinkel. 2011. Characterization of extracellular circulating microRNA. *Nucleic Acids Res.* 39: 7223–7233.
25. Arroyo, J. D., J. R. Chevillet, E. M. Kroh, I. K. Ruf, C. C. Pritchard, D. F. Gibson, P. S. Mitchell, C. F. Bennett, E. L. Pogosova-Agadjanyan, D. L. Stirewalt, et al. 2011. Argonaute2 complexes carry a population of circulating microRNAs independent of vesicles in human plasma. *Proc. Natl. Acad. Sci. USA* 108: 5003–5008.
26. Turchinovich, A., A. G. Tonevitsky, and B. Burwinkel. 2016. Extracellular miRNA: a collision of two paradigms. *Trends Biochem. Sci.* 41: 883–892.
27. Fabbri, M., A. Paone, F. Calore, R. Galli, E. Gaudio, R. Santhanam, F. Lovat, P. Fadda, C. Mao, G. J. Nuovo, et al. 2012. MicroRNAs bind to Toll-like receptors to induce prometastatic inflammatory response. *Proc. Natl. Acad. Sci. USA* 109: E2110–E2116.
28. Lehmann, S. M., C. Krüger, B. Park, K. Derkow, K. Rosenberger, J. Baumgart, T. Trimbuch, G. Eom, M. Hinz, D. Kaul, et al. 2012. An unconventional role for miRNA: let-7 activates Toll-like receptor 7 and causes neurodegeneration. *Nat. Neurosci.* 15: 827–835.
29. Park, C. K., Z. Z. Xu, T. Berta, Q. Han, G. Chen, X. J. Liu, and R. R. Ji. 2014. Extracellular microRNAs activate nociceptor neurons to elicit pain via TLR7 and TRPA1. *Neuron* 82: 47–54.
30. Zou, L., Y. Feng, G. Xu, W. Jian, and W. Chao. 2016. Splenic RNA and MicroRNA mimics promote complement factor B production and alternative pathway activation via innate immune signaling. *J. Immunol.* 196: 2788–2798.
31. Feng, Y., H. Chen, J. Cai, L. Zou, D. Yan, G. Xu, D. Li, and W. Chao. 2015. Cardiac RNA induces inflammatory responses in cardiomyocytes and immune cells via Toll-like receptor 7 signaling. *J. Biol. Chem.* 290: 26688–26698.
32. Feng, Y., L. Zou, D. Yan, H. Chen, G. Xu, W. Jian, P. Cui, and W. Chao. 2017. Extracellular microRNAs induce potent innate immune responses via TLR7/MyD88-dependent mechanisms. *J. Immunol.* 199: 2106–2117.
33. Caserta, S., F. Kern, J. Cohen, S. Drage, S. F. Newbury, and M. J. Llewelyn. 2016. Circulating plasma microRNAs can differentiate human sepsis and systemic inflammatory response syndrome (SIRS). *Sci. Rep.* 6: 28006.
34. Kawai, T., O. Adachi, T. Ogawa, K. Takeda, and S. Akira. 1999. Unresponsiveness of MyD88-deficient mice to endotoxin. *Immunity* 11: 115–122.
35. Yamamoto, M., S. Sato, H. Hemmi, K. Hoshino, T. Kaisho, H. Sanjo, O. Takeuchi, M. Sugiyama, M. Okabe, K. Takeda, and S. Akira. 2003. Role of adaptor TRIF in the MyD88-independent toll-like receptor signaling pathway. *Science* 301: 640–643.
36. Zou, L., Y. Feng, Y. Li, M. Zhang, C. Chen, J. Cai, Y. Gong, L. Wang, J. M. Thurman, X. Wu, et al. 2013. Complement factor B is the downstream effector of TLRs and plays an important role in a mouse model of severe sepsis. *J. Immunol.* 191: 5625–5635.

37. Théry, C., S. Amigorena, G. Raposo, and A. Clayton. 2006. Isolation and characterization of exosomes from cell culture supernatants and biological fluids. *Curr. Protoc. Cell Biol.* Chapter 3: Unit 3.22.
38. Harboe, M., and T. E. Mollnes. 2008. The alternative complement pathway revisited. *J. Cell. Mol. Med.* 12: 1074–1084.
39. Terrasini, N., and V. Lionetti. 2017. Exosomes in critical illness. *Crit. Care Med.* 45: 1054–1060.
40. Janiszewski, M., A. O. Do Carmo, M. A. Pedro, E. Silva, E. Knobel, and F. R. Laurindo. 2004. Platelet-derived exosomes of septic individuals possess proapoptotic NAD(P)H oxidase activity: a novel vascular redox pathway. *Crit. Care Med.* 32: 818–825.
41. Azevedo, L. C., M. Janiszewski, V. Pontieri, M. A. Pedro, E. Bassi, P. J. Tucci, and F. R. Laurindo. 2007. Platelet-derived exosomes from septic shock patients induce myocardial dysfunction. *Crit. Care* 11: R120.
42. Essandoh, K., L. Yang, X. Wang, W. Huang, D. Qin, J. Hao, Y. Wang, B. Zingarelli, T. Peng, and G. C. Fan. 2015. Blockade of exosome generation with GW4869 dampens the sepsis-induced inflammation and cardiac dysfunction. *Biochim. Biophys. Acta* 1852: 2362–2371.
43. de Couto, G., R. Gallet, L. Cambier, E. Jaghatspanyan, N. Makkar, J. F. Dawkins, B. P. Berman, and E. Marbán. 2017. Exosomal microRNA transfer into macrophages mediates cellular postconditioning. *Circulation* 136: 200–214.
44. Ying, W., M. Riopel, G. Bandyopadhyay, Y. Dong, A. Birmingham, J. B. Seo, J. M. Ofrecio, J. Wollam, A. Hernandez-Carretero, W. Fu, et al. 2017. Adipose tissue macrophage-derived exosomal miRNAs can modulate in vivo and in vitro insulin sensitivity. *Cell* 171: 372–384.e12.
45. Zuo, L., W. Yue, S. Du, S. Xin, J. Zhang, L. Liu, G. Li, and J. Lu. 2017. An update: epstein-Barr virus and immune evasion via microRNA regulation. *Virol. Sin.* 32: 175–187.
46. Feng, Y., L. Zou, R. Si, Y. Nagasaka, and W. Chao. 2010. Bone marrow MyD88 signaling modulates neutrophil function and ischemic myocardial injury. *Am. J. Physiol. Cell Physiol.* 299: C760–C769.